Biointerface Research in Applied Chemistry
Open-Access Journal (ISSN: 2069-5837)

Article
Volume 13, Issue 3, 2023, 250
https://doi.org/10.33263/BRIAC133.250

Nitrogen-Containing Graphene for Electrochemical Sensing of Glucose

Jhuma Debbarma [1], Ranjit Debnath [1], Mitali Saha [1,*]

[1] Department of Chemistry, National Institute of Technology Agartala, Tripura-799046, India
* Correspondence: mitalichem71@gmail.com (M.S.);

Scopus Author ID 5779373600
Received: 23.03.2022; Accepted: 23.04.2022; Published: 8.06.2022

Abstract: N-containing graphene was an excellent candidate for sensing and biosensing because of its comparable atomic radius with that of carbon and the formation of strong bonds. Its presence influenced the atomic charge distribution on the graphene scaffold, thereby enhancing the electrochemical activity. Here, nitrogen-containing graphene (N-graphene) prepared from papaya seeds was used to fabricate the electrode for the electrochemical oxidation of glucose using cyclic voltammetry and amperometry studies. The fabricated electrode showed a good response (6s) towards electrochemical oxidation of glucose with a linear range of 50-800 mg/L (R^2=0.99369), the sensitivity of ~ 10.888 $\mu AM^{-1}cm^{-2}$ along with a detection limit of 0.9 μM. It efficiently determined the glucose concentration in three real samples (apple juice, coco-cola, and honey), which were found to be 2.06%, 4.21%, and 41%, respectively. Moreover, the electrode exhibited an acceptable reproducibility (RSD 7.6%), and the stability was observed as 82..6% of the initial value up to 15 days.

Keywords: N-Graphene; β–D glucose; cyclic voltammetry; amperometry; real sample analysis.

1. Introduction

The electrochemical sensors are standard sensors for the determination of various analytes, where the sensors display relatively low detection limits with enhanced response times, and these are cheaper than other sensor-based available detection mechanisms [1-15]. Due to the absence of intrinsic bandgap, the use of pristine graphene was quite restricted towards sensing, drug screening, delivery, electrocatalysis, etc., whereas the doped graphene materials were found to enhance the performances of electrochemical sensors [16-32]. This is because the electrochemically active sites can be induced by doping heteroatoms within the graphitic lattice, which favors the anchoring of functional moieties, activation, and adsorption of analytes and accelerates the charge transfer between electrode and analytes. Among all, the incorporation of nitrogen in the graphitic lattice was not only easy due to its comparable atomic size with carbon atoms and formation of strong bonds with each other but also found to enhance the charge carrier density by the involvement of p-electrons of nitrogen with the π-system of graphene [33-35]. It was also revealed from impedance spectroscopy and cyclic voltammetry measurements that the presence of nitrogen improved the ion diffusion and charge propagation of the graphene.

As reported in our earlier work, a few layers of N-graphene were successfully prepared in a controlled manner from papaya seeds at relatively low temperature without the use of an inert atmosphere, in contrast to CVD technique where the flow of nitrogen, high temperature,

and target substrate is required to avoid the multi-layer formation of graphene. The method also bypassed the use of graphite powder, toxic chemicals, and doping agents, as reported in most of the literature [36-38]. The synthesized N-graphene was utilized to fabricate the electrode to detect glucose under nonenzymatic conditions. The cyclic voltammetry and amperometry studies were carried out to determine standard glucose and real samples, namely apple juice, coco-cola, and honey, respectively, presented in scheme 1. The response of N-graphene towards electrochemical detection of glucose confirmed that it might compete with any other commercially available N-graphene for sensing glucose.

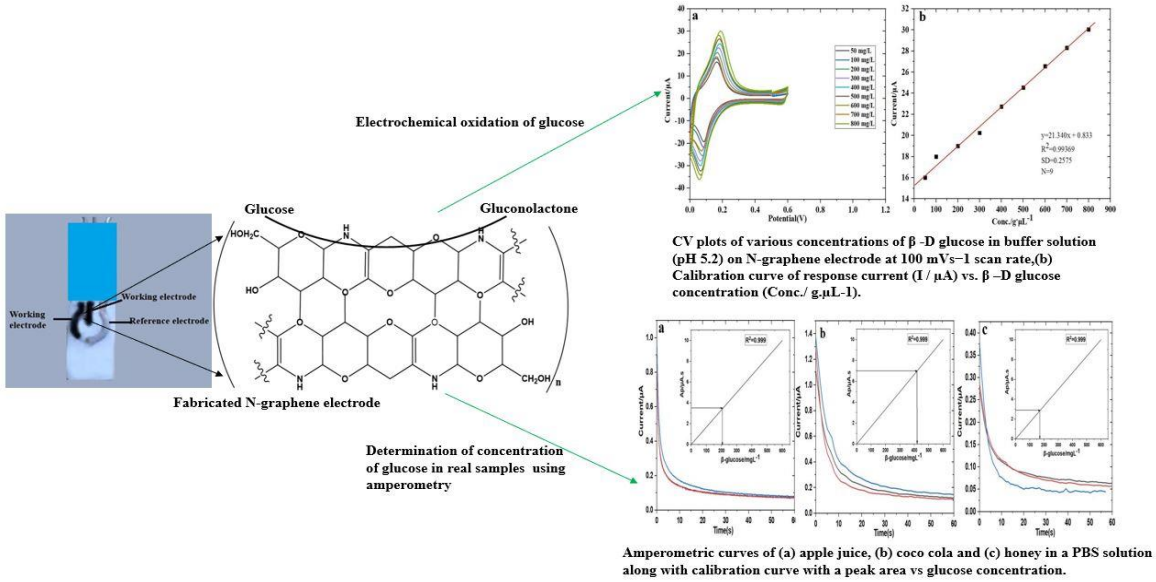

Scheme 1. Graphical abstract of electrochemical oxidation of glucose at fabricated N-graphene electrode.

2. Materials and Methods

D-(+)-glucose anhydrous ($C_6H_{12}O_6$), sodium hydrogen phosphate (Na_2HPO_4), potassium dihydrogen phosphate (KH_2PO_4), potassium chloride (KCl), and 99.999 % pure silver wires were purchased from Sigma. Silver wires were used to fabricate the N-graphene electrode. Potassium ferricyanide ($K_3[Fe(CN)_6]$), polystyrene, and chloroform were purchased from merk. Electrochemical studies were performed using a mini 910 PSTAT (Ω Metrohm), where a screen-printed CNT electrode was used as a standard electrode. Buffer solution (100 ml) was prepared by mixing 0.816 g KH_2PO_4, 0.099 g Na_2HPO_4, and 0.745 g KCl in 100 ml of deionized water and kept at 4 ºC before use. The stock solution of β-D glucose in 100 ml was prepared by dissolving 1 g β-D glucose in buffer solution (pH 5.2) with gentle stirring. The glucose solutions of different concentrations were prepared by diluting the stock solution in buffer solution.

2.1. Fabrication of electrode using N-graphene prepared from papaya seeds.

As reported in our earlier work, N-graphene obtained from papaya seeds was used to fabricate the electrode [38]. The dimension of the electrode was 3.5 cm x 1.0 cm x 0.5 cm (length x width x height) and fabricated on an insulating Teflon material containing three silver wires. A dense N-graphene powder and polystyrene solution was prepared in chloroform and deposited as a fine thin film on the Teflon surface, which served as both working and counter electrodes. The silver wire was used as a reference electrode.

2.2. Standardization of screen-printed carbon nanotubes(std-CNT) electrode.

A cyclic voltammetry study was performed with screen printed std-CNT electrode at a scan rate of 100 mVs^{-1} using a standard solution of hexacyanoferrate (III) of 0.1 mol/L in the presence of ammonium acetate buffer (pH 4.6). The ratio of the cathodic to the anodic current was calculated.

2.34. Nonenzymatic electrochemical detection of glucose using N-graphene electrode.

Cyclic voltammetry (CV) and amperometry studies were carried out at fabricated N-graphene electrodes for nonenzymatic detection of β –D glucose. The effect of scan rate and time interval were examined by CV using 100 ml/L of glucose solution in phosphate buffer (pH=5.2). Further, different concentrations of glucose solutions (50-800 mg/L) were prepared in phosphate buffer to study the fabricated N-graphene electrode's linearity, detection limit, and sensitivity. The amperometric measurements of three real samples, viz., apple juice, coco-cola, and honey, prepared in phosphate buffer (0.1:10 ratio) were performed, and the current response was recorded for 60s. The determination of various parameters, viz. concentration, reproducibility, and stability of the fabricated N-graphene electrode was carried out. The calibration curves were plotted between peak area vs. glucose concentration to determine the concentration of glucose in all the real samples.

3. Results and Discussion

3.1. Fabrication and standardization of graphene electrode with screen-printed carbon nanotubes (std-CNT) electrode.

The fabricated N-graphene electrode has presented in Figure 1a. CV study was performed with an N-graphene electrode using 0.1 mol/L $[K_3Fe(CN)_6]$ in ammonium acetate buffer solution and was compared with the screen-printed standard (std-CNT) electrode at the scan rate of 100 mVs^{-1}. The peak potential was found to be nearly 0. 60 V, and the ratio of the cathodic current over the anodic current was close to 1 in both cases (Figure 1b). This result was in good agreement with the Nernst equation for one electron system. The electrochemical response of the N-graphene electrode was comparable to std-CNT, which indicated that the N-graphene electrode could also be utilized as electrode material for electrochemical studies.

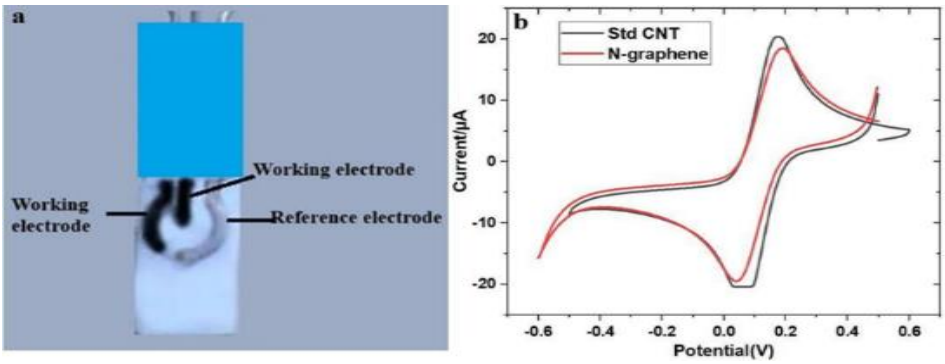

Figure 1. (a) Image of fabricated N-graphene electrode and (b) CV plots of 0.1 mol/L $[K_3Fe(CN)_6]$ in ammonium acetate buffer solution at 100 mVs^{-1} on the screen-printed std-CNT and prepared N-graphene electrode.

3.2. Effect of scan rate and time interval of glucose at graphene electrode.

The electrochemical oxidation of glucose on the fabricated N-graphene electrode was studied at the scan rate of 50-200 mVs^{-1} by CV using 100 mg/L glucose solutions. The CV

plots indicated that in the neutral PBS buffer, glucose oxidation into gluconolactone occurred at around +0.17 V (Figure 2a). The mechanism of preparation of N-graphene from papaya seeds and the electrochemical oxidation of glucose on the surface of the fabricated N-graphene electrode is presented in Figure 3. The current vs scan rate plot (Figure 2a$_1$) within the range of 50-200 mVs^{-1} showed a linear relationship between the peak intensity I(μA) and the scan rate (mVs^{-1}) via the linear regression equation I(μA) = 20.24 + 0.763 (mVs^{-1}) where, the correlation coefficient (R^2) was found to be 0.99986 along with standard deviation (SD) = 0.0447, N = 4. It indicated that the electrochemical kinetics reaction at the N-graphene electrode surface was an adsorption-controlled process. Furthermore, a plot of the logarithm of peak current vs. logarithm of scan rate gave a straight line with a slope of 0.944 (Figure 2a$_2$), which is close to the theoretical value of 1 for a purely adsorption-controlled process [39,40]. The linear regression equation was found to be, log I/μA = 1.07+ 0.944 log m/mVs^{-1} along with value of R^2 = 0.95945, standard deviation (SD) = 0.0388, N = 4.

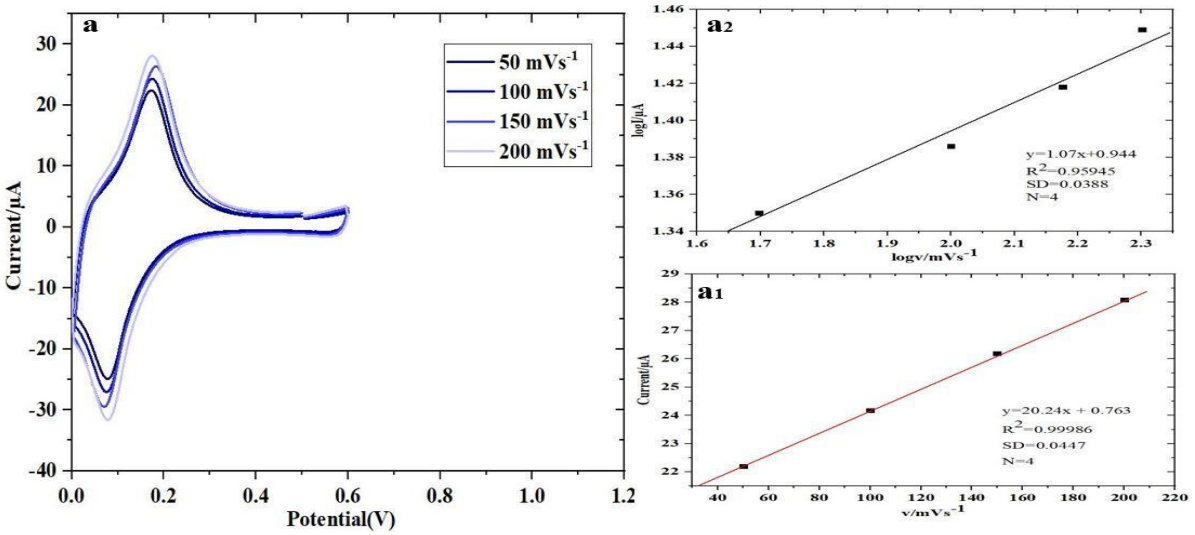

Figure 2. (a) CV plots of 100 mg/L β-D glucose in phosphate buffer solution at various scan rates (50,100,150, and 200 mVs^{-1}) on N-graphene electrode at pH 5.2 with (a$_1$) the plot of peak current (I/μA) vs. scan rate (ν/mVs^{-1}), (a$_2$) the plot of the logarithm of peak current vs. logarithm of scan rate.

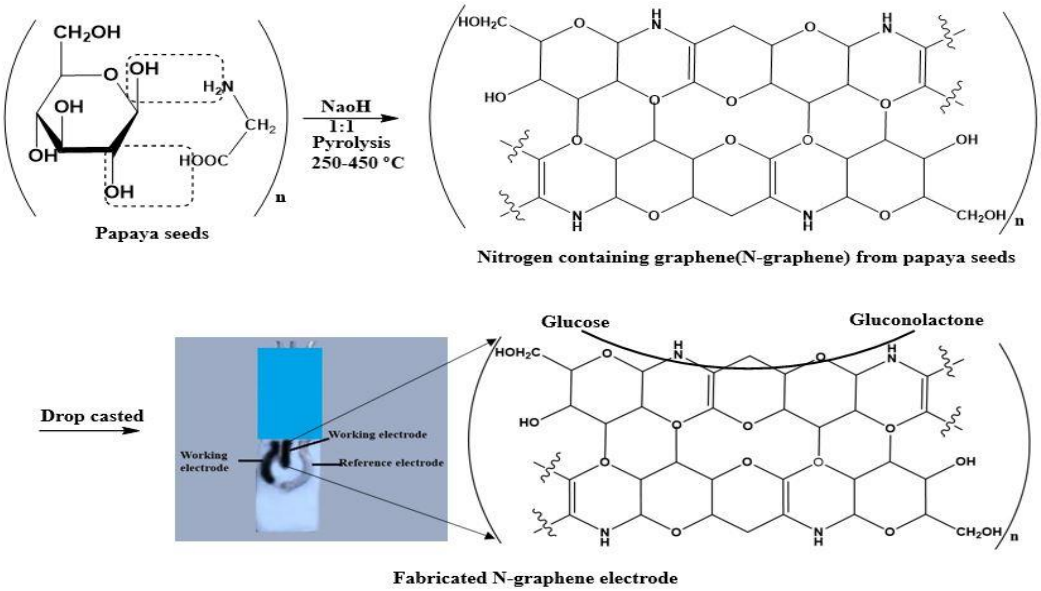

Figure 3. Electrochemical oxidation of glucose on the surface of fabricated N-graphene electrode.

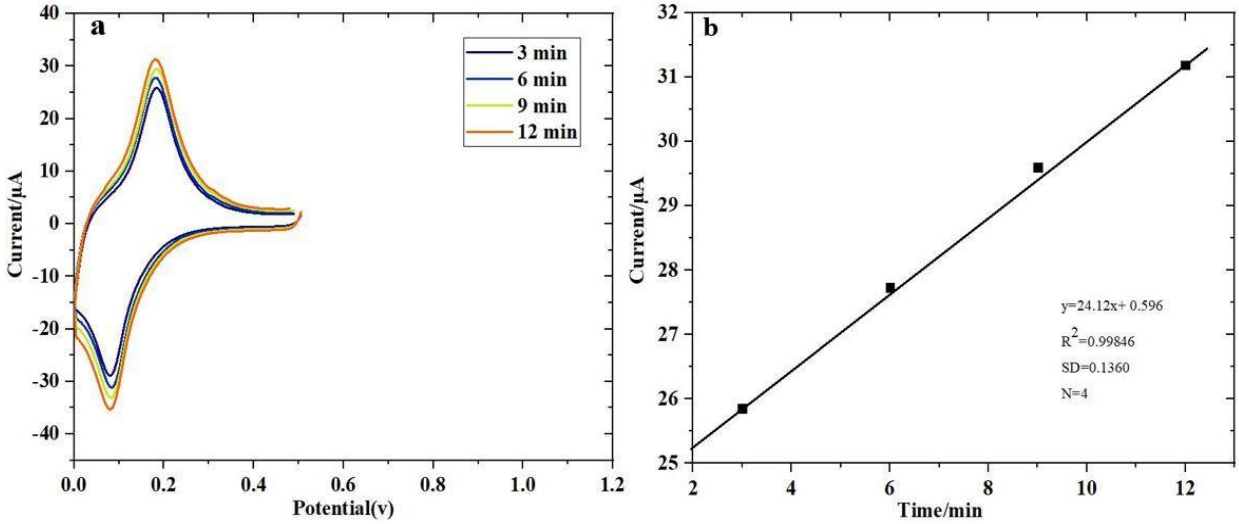

Figure 4. (a) CV plots of CV of 100 mg/L β-D glucose in phosphate buffer solution at various time intervals (3,6,9 and 12 min) at 100 mVs^{-1} scan rate on N-graphene electrode at pH 5.2 and (b) the plot of peak current (I /µA) vs. time interval (t/min).

The oxidation of glucose on the N-graphene electrode at different time intervals (3-12 min) was also studied at a fixed scan rate (100 mVs^{-1}), as presented in Figure 4a. The calibration plot (Figure 4b) showed good linearity between current and the time interval studies with a correlation coefficient (R^2) of 0.99846. The linear regression equation was found to be I /µA = 24.12+ 0.596 t/min. If the study was conducted over an extended time interval range (20 min), it resulted in a breakdown in the linearity relationship. This may be attributed that with the increase in time, the peak current gradually increased, but after 12 min, the peak current reached the maximum value and became stable.

3.3. Linearity, detection limit, and sensitivity of the graphene electrode.

CV was employed to determine the linearity, detection limit, and sensitivity of β –D glucose at fabricated N-graphene electrode using various glucose concentrations (50-800 mg/L) in PBS solution (pH 5.2) at a scan rate of 100 mVs^{-1}.

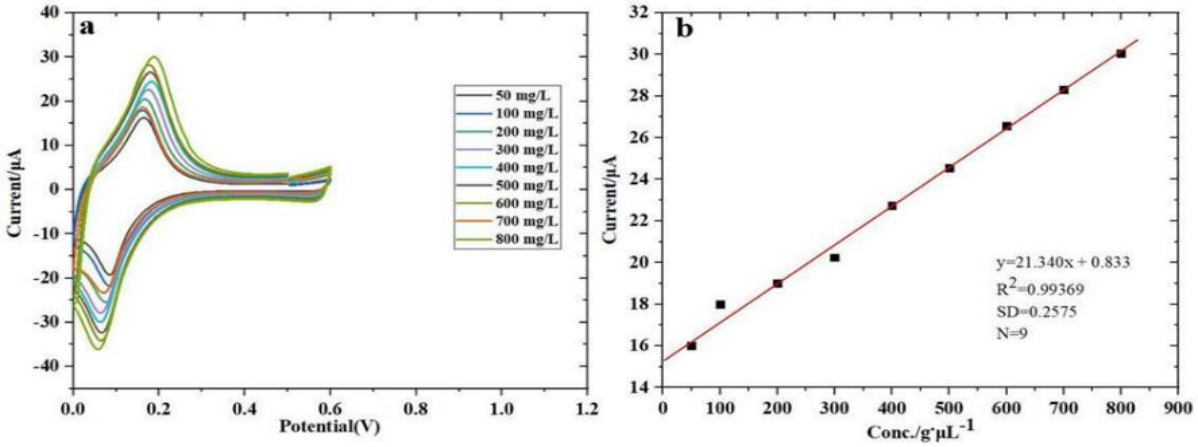

Figure 5. (a) CV plots of 50 – 800 mg/L of β -D glucose in buffer solution on N-graphene electrode at 100 mVs^{-1} scan rate (pH 5.2) and (b) calibration curve of response current (I/µA) vs. β–D glucose concentration (Conc./g.μL^{-1}).

It was observed that the peak current increased linearly with the increase of glucose concentrations, as presented in Figure 5a. From Figure 5b, it can be seen that the electrode showed good linearity in the glucose concentration range of 50-800 mg/L. The linear regression

equation for 50-800 mg/L of glucose concentrations was found to be, I/μA = 21.340 + 0.833 mg/L, where slope was 0.833. The correlation coefficient (R^2) value observed was 0.99369 for β–D glucose.

The active surface area of the N-graphene electrode was calculated using Randles–Sevcik equation.

$$IP = (2.69\times 10^5)\, n^{3/2} A D^{1/2} C \nu^{1/2}$$

where, n is the number of electrons participating in the redox reaction, A is the electroactive surface area (cm^2) of the electrode, D is the diffusion coefficient (cm^2s^{-1}), ν is the scan rate (mVs^{-1}), and C is the concentration of the redox probe molecule (mg/L). The active surface area of N-graphene electrode was found to be 0.0765 cm^2, where C = 0.1 M, D = 7.57 × 10^{-7} cm^2/s for $[Fe(CN)6]^{3-/4-}$ system. The sensitivity was calculated and found to be 10.888 $\mu A \mu M^{-1} cm^{-2}$ from the current versus concentration plot via slope/active surface area (Figure 3b). The limit of detection (LOD) and limit of quantification (LOQ) were calculated by the formulas LOD = 3s/m and LOQ = 10s/m, where s is the standard deviation of the peak currents and m is the slope of the calibration curve. The values were found to be 0.92 μM, and 3.09 μM, respectively, with the standard deviation(s) of the peak currents and slope(m) of the calibration curve found to be 0.2575 and 0.833, respectively.

3.4. Amperometric determination of glucose in real samples at graphene electrode.

Amperometric measurements were carried out to estimate the accuracy of the fabricated N-graphene electrode towards the determination of glucose concentration in three real samples, namely apple juice, coco-cola, and honey. Figure 6 (a-c) showed that a clear and rapid response of the N-graphene electrode was observed in the 60s, and a linear relationship existed between the glucose concentration (mg/L) and the peak area (Ap/μA. s) in each case. The concentration of glucose in all the samples was calculated using the volume correction method, i.e., C_{sample} = Csample solution V_{total}/V_{sample}, where, C_{sample} solution is the concentration in the sample solution, V_{total} is the total volume of the sample solution, Vsample is the volume of sample in the sample solution and C_{sample} is the concentration of glucose in the sample solution. The determination of glucose concentration of all the three samples using fabricated N-graphene electrodes was presented in Table 1. The experimental results were found to be comparable with those available in the literature [41-43]. The obtained results confirmed that the synthesized N-graphene prepared from papaya seeds may act as an electrode for glucose sensing.

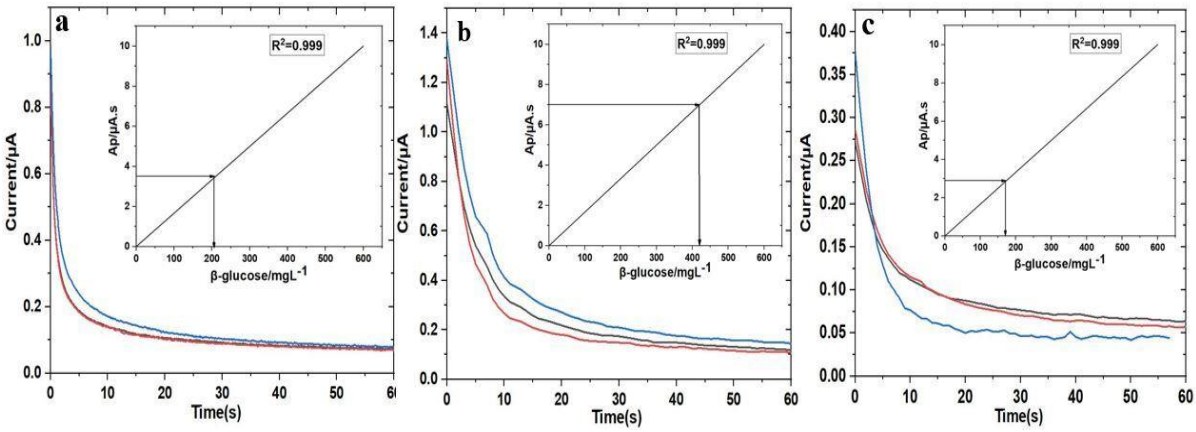

Figure 6. Amperometric curves of (a) apple juice, (b) coco-cola, and (c) honey in a PBS solution along with a calibration curve with a peak area vs. glucose concentration.

Table 1. Determination of glucose concentration in real samples at the N-graphene electrode

Sample	Reported glucose concentration (%)	Determination of glucose concentration (%)	RSD(%)
Apple juice	2.06	2.5	5.67
Coco cola	4.21	5	11.03
Honey	41	34.9	2.7

3.5. Repeatability and stability of fabricated graphene electrode.

The repeatability of the N-graphene electrode was determined by measuring the current responses of honey using 100 mg/L solutions in PBS (pH 5.2) solution, as presented in Figure 7(a). The experiments were carried out thrice using the same concentration of the honey solution. This showed a relative standard deviation (RSD) of 7.6 %, which indicated that the N-graphene electrode demonstrated acceptable repeatability and reusability. The electrode was also found to be stable, keeping 82.6 % of its initial value within a period of 15 days (Figure 7(b)).

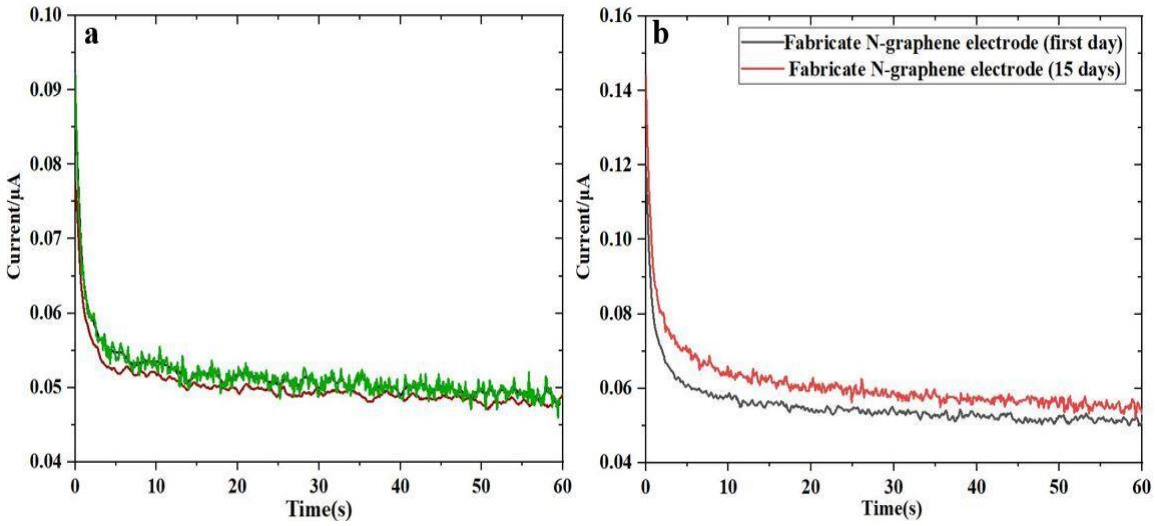

Figure 7. (a) Repeatability and (b) stability of fabricated N-graphene electrode.

4. Conclusions

N-graphene obtained from papaya seeds was used to fabricate the electrode to study the electrochemical oxidation of glucose under nonenzymatic conditions. Compared with other graphene-based nanocomposites, N-graphene prepared from pyrolysis at relatively low temperatures showed an excellent response toward glucose oxidation. When used for glucose sensing, it was observed that the fabricated N-graphene electrode possesses a sensitivity of 10.888 $\mu A \mu M^{-1} cm^{-2}$, a low detection limit of 0.92 µM, and good linearity within a glucose concentration range of 50-800 mg/L at pH 5.2. It also showed a rapid response of 6s with excellent stability of 82.6% of the initial value, up to 15 days. During amperometric determination in real samples (apple juice, coco-cola, and honey), the glucose concentrations were found to be comparable with the literature values. It confirmed that N-graphene prepared from papaya seeds might compete with commercially available N-graphene as electrode material for sensing glucose and other analytes.

Funding

This research received no external funding.

Acknowledgments

The authors are thankful to the Department of Chemistry, NIT Agartala.

Conflicts of Interest

The authors declare no conflict of interest.

References

1. Karimi-Maleh, H.; Yola, M.L.; Atar, N.; Orooji, Y.; Karimi, F.; Kumar, P.S.; Baghayeri, M. A novel detection method for organophosphorus insecticide fenamiphos: Molecularly imprinted electrochemical sensor based on core-shell Co3O4@ MOF-74 nanocomposite. *J. Colloid Interface Sci.* **2021**, *592*, 174-185, https://doi.org/10.1016/j.jcis.2021.02.066.
2. Naik, S.S.; Lee, S.J.; Theerthagiri, J.; Yu, Y.; Choi, M.Y. Rapid and highly selective electrochemical sensor based on ZnS/Au-decorated f-multi-walled carbon nanotube nanocomposites produced via pulsed laser technique for detection of toxic nitro compounds. *J. Hazard. Mater.* **2021**, *418*, https://doi.org/10.1016/j.jhazmat.2021.126269.
3. Kokulnathan, T.; Almutairi, G.; Chen, S.M.; Chen, T.W.; Ahmed, F.; Arshi, N.; Al Otaibi, B. Construction of lanthanum vanadate/functionalized boron nitride nanocomposite: the electrochemical sensor for monitoring of furazolidone. *ACS Sustain. Chem. Eng.* **2021**, *9*, 2784-2794, https://doi.org/10.1021/acssuschemeng.0c08340.
4. Xu, Z.; Wang, Q.; Zhangsun, H.; Zhao, S.; Zhao, Y.; Wang, L. Carbon cloth-supported nanorod-like conductive Ni/Co bimetal MOF: A stable and high-performance enzyme-free electrochemical sensor for determination of glucose in serum and beverage. *Food Chem.* **2021**, *349*, https://doi.org/10.1016/j.foodchem.2021.129202.
5. Huang, H.; Chen, Y.; Chen, Z.; Chen, J.; Hu, Y.; Zhu, J.J. Electrochemical sensor based on Ce-MOF/carbon nanotube composite for the simultaneous discrimination of hydroquinone and catechol. *J. Hazard. Mater.* **2021**, *416*, https://doi.org/10.1016/j.jhazmat.2021.125895.
6. Özcan, A.; Hamid, F.; Özcan, A.A. Synthesizing of a nanocomposite based on the formation of silver nanoparticles on fumed silica to develop an electrochemical sensor for carbendazim detection. *Talanta* **2021**, *222*, https://doi.org/10.1016/j.talanta.2020.121591.
7. Murugan, N.; Jerome, R.; Preethika, M.; Sundaramurthy, A.; Sundramoorthy, A.K. 2D-titanium carbide (MXene) based selective electrochemical sensor for simultaneous detection of ascorbic acid, dopamine and uric acid. *J Mater Sci Technol.* **2021**, *72*, 122-131, https://doi.org/10.1016/j.jmst.2020.07.037.
8. Huang, S.; Zhang, L.; Dai, L.; Wang, Y.; Tian, Y. Nonenzymatic electrochemical sensor with ratiometric signal output for selective determination of superoxide anion in rat brain. *Anal. Chem.* **2021**, *93*, 5570-5576, https://doi.org/10.1021/acs.analchem.1c00151.
9. Zhao, K.; Ge, L.; Wong, T.I.; Zhou, X.; Lisak, G. Gold-silver nanoparticles modified electrochemical sensor array for simultaneous determination of chromium (III) and chromium (VI) in wastewater samples. *Chemosphere* **2021**, *281*, https://doi.org/10.1016/j.chemosphere.2021.130880.
10. Ilager, D.; Shetti, N.P.; Malladi, R.S.; Shetty, N.S.; Reddy, K.R.; Aminabhavi, T.M. Synthesis of Ca-doped ZnO nanoparticles and its application as highly efficient electrochemical sensor for the determination of anti-viral drug, acyclovir. *J. Mol. Liq.* **2021**, *322*, https://doi.org/10.1016/j.molliq.2020.114552.
11. Ding, S.; Lyu, Z.; Li, S.; Ruan, X.; Fei, M.; Zhou, Y.; Lin, Y. Molecularly imprinted polypyrrole nanotubes based electrochemical sensor for glyphosate detection. *Biosens. Bioelectron.* **2021**, *191*, https://doi.org/10.1016/j.bios.2021.113434.
12. Patella, B.; Russo, R.R.; O'Riordan, A.; Aiello, G.; Sunseri, C.; Inguanta, R. Copper nanowire array as highly selective electrochemical sensor of nitrate ions in water. *Talanta* **2021**, *221*, https://doi.org/10.1016/j.talanta.2020.121643.
13. Chu, N.; Liang, Q.; Hao, W.; Jiang, Y.; Liang, P.; Zeng, R.J. Microbial electrochemical sensor for water biotoxicity monitoring. *Chem. Eng. J.* **2021**, *404*, https://doi.org/10.1016/j.cej.2020.127053.
14. Saeb, E.; Asadpour-Zeynali, K. Facile synthesis of TiO2@ PANI@ Au nanocomposite as an electrochemical sensor for determination of hydrazine. *Microchem. J.* **2021**, *160*, https://doi.org/10.1016/j.microc.2020.105603.
15. Carneiro, L.P.; Ferreira, N.S.; Tavares, A.P.; Pinto, A.M.; Mendes, A.; Sales, M.G.F. A passive direct methanol fuel cell as transducer of an electrochemical sensor, applied to the detection of carcinoembryonic antigen. *Biosens. Bioelectron.* **2021**, *175*, https://doi.org/10.1016/j.bios.2020.112877.
16. de Sousa, M.; Visani de Luna, L.A.; Fonseca, L.C.; Giorgio, S.; Alves, O.L. Folic-acid-functionalized graphene oxide nanocarrier: synthetic approaches, characterization, drug delivery study, and antitumor screening. *ACS Appl. Nano Mater.* **2018**, *1*, 922-932, https://doi.org/10.1021/acsanm.7b00324.

17. Lee, J.M.; Park, D.Y.; Yang, L.; Kim, E.J.; Ahrberg, C.D.; Lee, K.B.; Chung, B.G. Generation of uniform-sized multicellular tumor spheroids using hydrogel microwells for advanced drug screening. *Sci. Rep.* **2018**, *8*, 1-10, https://doi.org/10.1038/s41598-018-35216-7.
18. Castrignano, S.; Gilardi, G.; Sadeghi, S.J. Human flavin-containing monooxygenase 3 on graphene oxide for drug metabolism screening. *Anal. Chem.* **2015**, *87*, 2974-2980, https://doi.org/10.1021/ac504535y.
19. Song, J.; Li, Y.; Yin, F. Enhanced electrochemical impedance spectroscopy analysis of microbial biofilms on an electrochemically in situ generated graphene interface. *ACS Sens.* **2020**, *5*, 1795-1803, https://doi.org/10.1021/acssensors.0c00570.
20. Xiong, X.; Chen, Y.; Wang, H.; Hu, S.; Luo, Y.; Dong, J.; Chen, Z. Plasmonic interface modified with graphene oxide sheets overlayer for sensitivity enhancement. *ACS Appl. Mater.* **2018**, *10*, 34916-34923, https://doi.org/10.1021/acsami.8b11424.
21. Madni, A.; Noreen, S.; Maqbool, I.; Rehman, F.; Batool, A.; Kashif, P.M.; Khan, M.I. Graphene-based nanocomposites: synthesis and their theranostic applications. *J. Drug Target.* **2018**, *26*, 858-883, https://doi.org/10.1080/1061186X.2018.1437920.
22. Rahmanian, N.; Eskandani, M.; Barar, J.; Omidi, Y. Recent trends in targeted therapy of cancer using graphene oxide-modified multifunctional nanomedicines. *J. Drug Target.* **2017**, *25*, 202-215, https://doi.org/10.1080/1061186X.2016.1238475.
23. Liu, J.; Cui, L.; Losic, D. Graphene and graphene oxide as new nanocarriers for drug delivery applications. *Acta Biomater.* **2013**, *9*, 9243-9257, https://doi.org/10.1016/j.actbio.2013.08.016.
24. Pan, Y.; Sahoo, N.G.; Li, L. The application of graphene oxide in drug delivery. *Expert Opin Drug Deliv.* **2012**, *9*, 1365-1376, https://doi.org/10.1517/17425247.2012.729575.
25. Weaver, C.L.; LaRosa, J.M.; Luo, X.; Cui, X.T. Electrically controlled drug delivery from graphene oxide nanocomposite films. *ACS nano.* **2014**, *8*, 1834-1843, https://doi.org/10.1021/nn406223e.
26. Daniyal, M.; Liu, B.; Wang, W. Comprehensive review on graphene oxide for use in drug delivery system. *Curr. Med. Chem.* **2020**, *27*, 3665-3685, https://doi.org/10.2174/1381612825666190201129629O.
27. Xia, B.; Yan, Y.; Wang, X.; Lou, X.W.D. Recent progress on graphene-based hybrid electrocatalysts. *Mater. Horiz.* **2014**, *1*, 379-399, https://doi.org/10.1039/C4MH00040D.
28. Zhang, X.; Gao, J.; Xiao, Y.; Wang, J.; Sun, G.; Zhao, Y.; Qu, L. Regulation of 2D graphene materials for electrocatalysis. *Chem. Asian J.* **2020**, *15*, 2271-2281, https://doi.org/10.1002/asia.202000249.
29. Tung, T.T.; Nine, M.J.; Krebsz, M.; Pasinszki, T.; Coghlan, C.J.; Tran, D.N.; Losic, D. Recent advances in sensing applications of graphene assemblies and their composites. *Adv. Funct. Mater.* **2017**, *27*, https://doi.org/10.1002/adfm.201702891.
30. Duan, J.; Chen, S.; Jaroniec, M.; Qiao, S.Z. Heteroatom-doped graphene-based materials for energy-relevant electrocatalytic processes. *ACS Catal.* **2015**, *5*, 5207-5234, https://doi.org/10.1021/acscatal.5b00991.
31. Jiao, Y.; Zheng, Y.; Davey, K.; Qiao, S.Z. Activity origin and catalyst design principles for electrocatalytic hydrogen evolution on heteroatom-doped graphene. *Nat. Energy*. **2016**, *1*, 1-9, https://doi.org/10.1038/nenergy.2016.130.
32. Wang, Y.; Shao, Y.; Matson, D.W.; Li, J.; Lin, Y. Nitrogen-doped graphene and its application in electrochemical biosensing. *ACS nano*. **2010**, *4*, 1790-1798, https://doi.org/10.1021/nn100315s.
33. Sun, L.; Wang, L.; Tian, C.; Tan, T.; Xie, Y.; Shi, K.; Fu, H. Nitrogen-doped graphene with high nitrogen level via a one-step hydrothermal reaction of graphene oxide with urea for superior capacitive energy storage. *Rsc Adv.* **2012**, *2*, 4498-4506, https://doi.org/10.1039/C2RA01367C.
34. Jeong, H.M.; Lee, J.W.; Shin, W.H.; Choi, Y.J.; Shin, H.J.; Kang, J.K.; Choi, J.W. Nitrogen-doped graphene for high-performance ultracapacitors and the importance of nitrogen-doped sites at basal planes. *Nano Lett.* **2011**, *11*, 2472-2477, https://doi.org/10.1021/nl2009058.
35. Wang, H.; Maiyalagan, T.; Wang, X. Review on recent progress in nitrogen-doped graphene: synthesis, characterization, and its potential applications. *ACS Catal.* **2012**, *2*, 781-794, https://doi.org/10.1021/cs200652y.
36. Wei, D.; Liu, Y.; Wang, Y.; Zhang, H.; Huang, L.; Yu, G. Synthesis of N-doped graphene by chemical vapor deposition and its electrical properties. *Nano Lett.* **2009**, *9*, 1752-1758, https://doi.org/10.1021/nl803279t.
37. Sheng, Z.H.; Shao, L.; Chen, J.J.; Bao, W.J.; Wang, F.B.; Xia, X.H. Catalyst-free synthesis of nitrogen-doped graphene via thermal annealing graphite oxide with melamine and its excellent electrocatalysis. *ACS nano* **2011**, *5*, 4350-4358, https://doi.org/10.1021/nn103584t.
38. Debbarma, J.; Mandal, P.; Saha, M. Fruit wastes to N-containing graphene: chemistry and mechanism. *Fuller Nanotub Car N.* **2021**, *29*, 1-7, https://doi.org/10.1080/1536383X.2021.1889517.
39. Gosser, D.K. *Cyclic voltammetry: simulation and analysis of reaction mechanisms*. New York: VCH. 1993; 154, https://doi.org/10.1080/00945719408001398.
40. Bard, A.J.; Faulkner, L.R. Fundamentals and applications. *Electrochem. Methods.* **2001**, *2*, 580-632.
41. Shi, R.; Stein, K.; Schwedt, G. Spectrophotometric determination of glucose in foods by flow injection analysis with an immobilized glucose oxidase reactor. *Zeitschrift für Lebensmitteluntersuchung und-Forschung A* **1997**, *204*, 99-102, https://doi.org/10.1007/s002170050044.

42. Meurman, J.H.; Rytömaa, I.; Kari, K.; Laakso, T.; Murtomaa, H. Salivary pH and glucose after consuming various beverages, including sugar-containing drinks. *Caries Res.* **1987**, *21*, 353-359, https://doi.org/10.1159/000261039.
43. Wahdan, H.A.L. Causes of the antimicrobial activity of honey. *Infection* **1998**, *26*, 26-31, https://doi.org/10.1007/BF02768748.